A mixing length model for
estimating channel conveyance

[1] **Matthew S. Horritt** PhD, CEng, CWEM, MCIWEM
Consulting Environmental Engineer, Bristol, UK

[2] **Nigel G. Wright** PhD, CEng, FASCE, FHEA, FICE
Professor of Water and Environmental Engineering, University of
Leeds, Leeds, UK

This paper describes a simple, physically based mixing length model that explains the functional form of Manning's
equation for mean velocity in open channels. Manning's equation has been used to describe mean velocity for over
100 years and is essentially an empirical result rather than being based on an understanding of physical processes.
The model described in this paper uses Prandtl's mixing length hypothesis, with mixing length modelled at each
point within the cross-section being proportional to the distance to the nearest solid boundary. The model solves
equations for the along-stream velocity field using a simple numerical method on regular and irregular finite-
difference meshes. The results of the model are compared with Manning's equation and the Colebrook–White
formula, giving good agreement across a range of channel sizes, roughnesses and geometries. The results and
comparison are used to draw useful insights into open channel flows.

Notation

a, b, c, d	weights of neighbouring points used in averaging in Jacobi's method
dx^+, dx^-, etc.	forward and backward difference grid spacings, values for y are defined similarly
g	acceleration due to gravity
h	depth of flow
h_0	distance above bed at which velocity goes to zero
k_s	bed material grain size
l	mixing length
n	Manning's coefficient of resistance
n'	generalised Manning's coefficient of resistance
R	hydraulic radius
Re	Reynolds number
r	distance from centre of circular channel
S	along-stream channel slope
u	along-stream velocity component
u^*	shear velocity
u_0 and u_1	velocities calculated at point nearest the bed and the point one above
v	cross-section average velocity
v_x, v_y	turbulent eddy viscosity for velocity gradients in x and y directions
x, y, z	distance along stream, horizontally across stream and vertically, respectively
α	ratio of velocities at point nearest the bed and the one above
γ	power of R in generalised Manning's equation
Δz	vertical grid spacing for wall function model
κ	von Karman's constant
ρ	density of water
τ	shear stress
τ_b	bed shear stress

1. Introduction

Manning's equation, and related equations such as the Chezy and Strickler equations, have been used by engineers for over 100 years to estimate the capacity of open channels to convey water. Manning's equation describes the relationship between the cross-section average water velocity v, the bed slope S, the hydraulic radius R and a resistance coefficient n for uniform, steady flows

1. $$v = \frac{1}{n} R^{2/3} S^{1/2}$$

The form of this equation raises two questions.

Firstly, why is the velocity dependent on the hydraulic radius? Intuitively, this is sensible: the hydraulic radius describes the ratio of the amount of water in the channel (and hence its weight) to the length of wall in contact with the water. The

hydraulic radius is a characteristic of the geometry and thus a simple way of incorporating the cross-section geometry in the model (Chanson, 1999; Morvan *et al.*, 2008). However, it is not clear why this simple combination of area and perimeter should control the velocity, rather than some other, more complex relationship.

Secondly, why the 2/3 power? The 2/3 power was derived by Manning from an analysis of results from a number of other researchers in the eighteenth and nineteenth centuries, and the dimensional inconsistency of the equation troubled Manning enough for him to reformulate the equation in a more complex but dimensionally consistent way (Manning, 1891). Engineers, however, persisted with the simpler form. There is no intuitive explanation of why a 2/3 power should appear in an equation describing channel flow.

The Manning equation as applied to uniform flow conditions implies that the water surface slope, and therefore the bed shear stress, is proportional to v^2. This is similar to many other situations in hydrodynamics where the flow resistance is proportional to v^2, and therefore the dependence between S and v is as expected. In contrast, the dependence on R by a 2/3 power rather than any other power is essentially an empirical result. Indeed, Chezy's equation also uses the hydraulic radius, but with a different power. What hydraulic processes generate this dependence?

Previous work on modelling steady, uniform flow in open channel cross-sections has tended to focus on representing complex cross-sections and the effects of turbulence and horizontal velocity variations on conveyance. Shiono and Knight (1991) use a simplification of the shallow-water equations to model conveyance in a cross-section divided into a series of panels. This approach has been used practically in the conveyance estimation system (McGahey *et al.*, 2008). A finite-element method has been used to model conveyance (Abril and Knight, 2004; Knight and Abril, 1996) in complex cross-sections, and a one-dimensional (1D) across the channel model has been used to understand the effects of vegetation (Darby and Thorne, 1996). The research reported in these references does not, however, attempt to explain why a relationship like those of Manning or Chezy works in describing conveyance, but instead tries to extend its validity to more complex situations.

This paper describes a simple mixing length model that can reproduce the known conveyance behaviour of open channels, based on physical arguments rather than empirical results. This behaviour is reproduced by the Manning and Chezy equations, meaning that the results of the mixing length model are compatible with well-understood engineering approaches to conveyance estimation, but also offering an insight into why these behaviours occur. As well as providing some insight into how the functional dependencies in the equation arise, the model may be of practical use in modelling conveyance in open channels, with applications in river engineering, water resources and flood modelling.

2. Two-dimensional mixing length model

The mixing length model of Prandtl (Prandtl, 1945; Schlichting *et al.*, 2004) was developed as a simple way of providing analytically tractable closures for turbulent flows. By analogy with the relationship between molecular viscosity in gases and the molecular mean free path, Prandtl hypothesised that the shear stress generated by turbulent mixing could be written in terms of a mixing length l

2.
$$\tau = \rho l^2 \left(\frac{\mathrm{d}u}{\mathrm{d}y}\right)^2$$

The shear stress τ is related to the mixing length l, the velocity profile (written here for a velocity u varying only in the y direction) and density ρ. The mixing length describes the distance a parcel of fluid tends to travel in a cross-stream direction before becoming homogenised with the surrounding fluid. A longer mixing length means that fluid will travel further, and hence transport momentum from further away, increasing mixing and producing a larger shear stress. Another way of thinking of the mixing length is in terms of the size of the eddies that transport momentum and other properties (temperature, solute concentration) within a fluid. The application of a mixing length model in channel flows is attractive because it is capable of reproducing the observed logarithmic velocity profile near rough walls and because it is intuitively simple. By modelling the mixing length as a proportion of the distance to the wall, the observed hydraulic behaviour can be reproduced. The constant of proportionality is von Karman's constant κ, which has been empirically determined as 0·41 for many flows and is consistent with current understanding of the fundamental properties of turbulence (Lo *et al.*, 2005). Thus, mixing is limited near the wall, where large eddies will be disrupted by interaction with the solid boundary, and mixing increases away from the wall where larger eddies can form.

Extension of the 1D mixing length model to more complex channel shapes is straightforward (but the solution of the resulting equations is sometimes difficult). Assuming uniform, steady flow, the stress in a fluid is generated by vertical and horizontal shear. Considering velocity variations in the cross-stream (y) and vertical directions (z), and assuming steady, uniform flow in the x direction, the Reynolds averaged Navier–Stokes momentum equation becomes

3.
$$\rho \boldsymbol{g} S + \frac{\partial \tau_{xy}}{\partial y} + \frac{\partial \tau_{xz}}{\partial z} = 0$$

The weight of the fluid is thus balanced by vertical and horizontal

shear stress gradients. Based on Prandtl's theory, these stresses can be written as

$$
\tau_{xy} = \rho l^2 |\nabla u| + \frac{\partial u}{\partial y}
$$

4.
$$
\tau_{xz} = \rho l^2 |\nabla u| + \frac{\partial u}{\partial z}
$$

in which u is the Reynolds average velocity component in the x (along stream) direction and assuming that molecular viscosity can be neglected for a fully turbulent flow. Differentiating the shear stresses gives

$$
\frac{\partial \tau_{xy}}{\partial y} = \rho l^2 |\nabla u| + \frac{\partial^2 u}{\partial y^2} + \rho l^2 \frac{\partial |\nabla u|}{\partial y} \frac{\partial u}{\partial y}
$$

5.
$$
+ 2\rho l \frac{\partial l}{\partial y} |\nabla u| \frac{\partial u}{\partial y}
$$

A similar equation can be written for the derivative of τ_{xz} with respect to z. The derivative of the magnitude of the velocity gradient in the second term is (assuming velocity is constant in the x direction)

6.
$$
\frac{\partial |\nabla u|}{\partial y} = \frac{1}{|\nabla u|} \left(\frac{\partial u}{\partial y} \frac{\partial^2 u}{\partial y^2} + \frac{\partial u}{\partial z} \frac{\partial^2 u}{\partial y \partial z} \right)
$$

The terms from Equations 4, 5 and 6 can be grouped into terms involving second derivatives with respect to x and y, and source terms

$$
\left[\rho l^2 |\nabla u| + \frac{\rho l^2}{|\nabla u|} \left(\frac{\partial u}{\partial y} \right)^2 \right] \frac{\partial^2 u}{\partial y^2}
$$

$$
+ \left[\rho l^2 |\nabla u| + \frac{\rho l^2}{|\nabla u|} \left(\frac{\partial u}{\partial z} \right)^2 \right] \frac{\partial^2 u}{\partial z^2}
$$

$$
+ \rho \boldsymbol{g} S + 2 \frac{\rho l^2}{|\nabla u|} \frac{\partial^2 u}{\partial y \partial z} \frac{\partial u}{\partial z} \frac{\partial u}{\partial y}
$$

7.
$$
+ 2\rho l |\nabla u| \left(\frac{\partial l}{\partial y} \frac{\partial u}{\partial y} + \frac{\partial l}{\partial z} \frac{\partial u}{\partial z} \right) = 0
$$

This gives the 2D Poisson equation, with inhomogeneous coefficients, and source terms arising from the component of the weight of water in the along-stream direction and derivative terms. The different coefficients of the second derivatives in y and z mean that the eddy viscosity is anisotropic. These equations

are solved by the methods described in the following sections to produce the results presented in this paper.

The boundary conditions for this problem are applied at the bed and free surface. At the bed, the boundary condition is that the velocity is zero at a distance h_0 from the wall or bed. This distance is not zero and can be thought of as a factor to set the mixing length near the bed. This controls the velocity distribution in the rest of the channel by determining the mixing length and hence the velocity gradient at the point near the bed where the velocity goes to zero. The distance h_0 is thus a way of parameterising a boundary condition for the mixing length model near the bed. The boundary condition at the horizontal free surface is that the vertical shear stress τ_{xz} should be zero. It is recognised that the treatment of the free surface boundary condition here is simplistic and that the assumption of isotropic turbulence is not entirely valid. Rodi (1993) develops a surface boundary condition that more realistically represents observed eddy behaviour near the free surface. However, in terms of a comparison with Manning and Chezy, this is not felt to be significant as the main influence on conveyance is the behaviour near the bed and walls rather than near the surface where velocity gradients are smaller.

The final link with Manning's equation concerns the relationship between Manning's coefficient n, h_0 and the roughness height describing the geometric properties of the walls and bed. For bed and walls composed of uniform grain size k_s, the zero-velocity depth h_0 will be equal to $0.033k_s$, according to experiments undertaken by Nikuradse (1933). This provides a link between the geometric properties of the bed and the velocity profile, as controlled by h_0. The equation $h_0 = 0.033k_s$ describes the relationship between the grain size and the initial mixing length as discussed above.

This relationship assumes that the flow is hydraulically rough; that is, there is turbulent flow in the boundary layer near the bed. A link between the roughness height k_s and Manning's resistance is provided by the Colebrook–White equation (Colebrook, 1939), a relationship between velocity, hydraulic radius, roughness height and slope for laminar, transitional and turbulent flows

8.
$$
v = -(8\boldsymbol{g}RS)^{1/2} 2\log_{10} \left[\frac{2 \cdot 51}{\text{Re}} \left(\frac{v^2}{8\boldsymbol{g}RS} \right)^{1/2} + \frac{k_s}{12 \cdot 3R} \right]
$$

This relationship is based on the Prandtl mixing length hypothesis and dimensional analysis and uses experimental results to fit the relationship to observations. A range of values for the parameters in this equation has been found by fitting to experimental data for closed pipes and open channels of different geometries (Yen, 1991); a commonly used median value is used here. For turbulent flows with high Reynolds number Re, the first term of the logarithm can be ignored, giving a simple relationship that does

not require an iterative solution for v. As is known, the Colebrook–White equation and Manning's equation are not equivalent, but give similar results when compared for limited ranges of the hydraulic radius. If the Colebrook–White equation is taken as applicable, it implies that Manning's n is a weak function of depth.

For the results presented in this paper, the mixing length at each point in the cross-section is modelled as simply the distance to the nearest point on the bed or wall, multiplied by von Karman's constant. The distance is calculated explicitly by the model between each computational point and the walls and bed. This splits the channel into zones of influence from bed and walls (De Cacqueray *et al.*, 2009; Morvan *et al.*, 2008), and the mixing length varies within the cross-section according to the distance to the nearest solid boundary. The hydraulics are determined therefore by the distance to the point that would be expected to be most significant in generating local shear.

This relationship between mixing length and geometry has two advantages. Firstly, it will reproduce the observed (approximately) logarithmic velocity profiles in regions of approximately constant shear stress near the bed and walls. Secondly, it allows us to relate horizontal and vertical momentum mixing processes. For example, we would not expect eddies to transport momentum a large distance horizontally in shallow flows, where these eddies would be disrupted by the vertical velocity shear. In deeper flows, larger eddies would be expected and hence greater horizontal mixing should occur. The length scales over which momentum can be transported across vertical and horizontal velocity gradients are thus linked. This may be important for open channel flows in natural rivers, where shear layers have been observed to form between the channel and floodplain. Assuming that the horizontal mixing length is approximately equal to the depth may be a simple way of estimating the effects of these shear layers.

The authors have developed various solution methods for different geometries, as described below. The solutions have been implemented using the Python high-level language on a standard PC. While Python is not ideal in terms of speed for numerical solutions, it does allow rapid development of code to test the various solution methods. Faster solutions could doubtless be implemented in C/C++ or other lower level languages.

2.1 One-dimensional Runge–Kutta solution for planar beds and circular conduits

The solution of Equations 3 and 4 for planar beds can be much simplified because the shear stress in the water column is known exactly and is equal to the component of the weight of water above that point

9.
$$\tau_{xz} = \rho l^2 \left| \frac{\partial u}{\partial z} \right| \frac{\partial u}{\partial z} = \rho \mathbf{g} S(h - z)$$

where h is the water depth. The mixing length model is now a first-order initial value problem, with the initial value derived from the bed boundary condition that the velocity is zero at a known distance above the bed. No surface boundary condition is required, as this is implicit in the specification of the shear stress, which goes to zero at the free surface.

Equation 9 can be easily solved using the standard fourth-order Runge–Kutta solution (Press *et al.*, 2007), with the first calculation point set at the roughness height h_0. A step size of 1 mm was used here, as the solution method is fast enough to allow the use of a very fine grid. A small grid spacing is required to capture the steep velocity gradients near the bed and this is crucial in determining the velocity profile in the rest of the water column.

The 1D solution can be easily adapted to model flow in circular conduits with full flow

10.
$$\tau_{xr} = \rho l^2 \left| \frac{\partial u}{\partial r} \right| \frac{\partial u}{\partial r} = \frac{\rho \mathbf{g} S r}{2}$$

The shear stress here can be written in this way by considering the weight of water in a circular region of radius r, which is balanced by the shear stress acting over a length $2\pi r$. The functional form of the solution is therefore the same as for the planar bed (since $r = h - z$), but with the slope halved. The circular shape of the channel must also be considered when the solution is integrated to give the section average flow.

2.2 Two-dimensional solution for rectangular channels

The form of Equation 7 suggests that the Jacobi method may be used, as it is well known to produce stable (albeit slow) convergence for the Laplace and Poisson equations. Jacobi's method (Press *et al.*, 2007) provides a slowly converging, but robust and simple to implement, iterative method. It is usually applied to regular square grids, using finite-difference approximations to the second-order gradient terms. The value at a grid point is replaced by the mean of values at neighbouring points, plus source terms if required. Other numerical methods (e.g. Gauss–Seidel) may also be applicable – and faster – but the focus of this paper is the nature of the solutions rather than how they are derived and the speed of the algorithm is not too important for the simple geometries tested here.

The main difficulty in applying the Jacobi method to this problem is in specifying the grid size, since the numerical method used to solve the equations must be able to represent the variations in velocity near the bed and walls, which occur over short length scales (hence the use of the 1 mm grid size for the Runge–Kutta solution). A small grid size, would, however, be prohibitively slow to converge if applied to the whole cross-section.

For the results presented in this paper, a non-uniform grid spacing was therefore used, with points closer together near the bed,

where velocity gradients are steepest, and points more widely spaced further away from the walls and bed. While use of an irregular grid reduces accuracy (e.g. a centred difference approximation to a gradient is second-order accurate on a regular grid, but only first-order accurate on an irregular grid), the need to represent steep velocity gradients near the bed makes a regular grid impractical.

The vertical grid point positions are given by a geometric progression

11. $$z_0 = h_0, \quad z_{i+1} = z_i 10^{[\log 10(h/h_0)]/N}$$

Horizontal positions are defined similarly, with the same ratio between point positions, and with the spacing increasing to a maximum in the centre of the channel then decreasing again towards the right-hand wall. The grid points for a rectangular cross-section are shown in Figure 1. The $10^{(\ldots)}$ term can be viewed as a grid spacing increment factor, as it determines how much the grid spacing increases between neighbouring cells.

Implementation of the Jacobi method requires finite-difference approximations adapted to work with an irregular grid. The iteration formula is derived by considering the finite-difference approximation to the ∇^2 operator, and the new value becomes a weighted mean of neighbouring points plus source terms

12. $$u_{i,j}^{t+1} = \frac{au_{i+1,j}^t + bu_{i-1,j}^t + cu_{i,j+1}^t + du_{i,j-1}^t}{a+b+c+d} + s_{i,j}$$

The superscript t represents the iteration number. a, b, c, and d depend on the local grid spacings and the anisotropic eddy
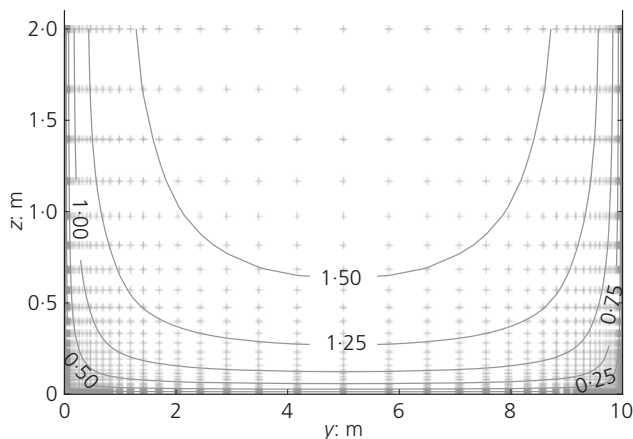
Figure 1. Velocity contours predicted by the mixing length model, using irregular grid spacing, for a rectangular channel with $k_s = 0.2$ m. Grid points are shown by crosses

viscosity and s is the source term (weight of water plus other terms from Equation 7)

$$a = \frac{\nu_y}{\mathrm{d}y^+(\mathrm{d}y^+ + \mathrm{d}y^-)}$$

$$b = \frac{\nu_y}{\mathrm{d}y^-(\mathrm{d}y^+ + \mathrm{d}y^-)}$$

$$c = \frac{\nu_z}{\mathrm{d}z^+(\mathrm{d}z^+ + \mathrm{d}z^-)}$$

13. $$d = \frac{\nu_z}{\mathrm{d}z^-(\mathrm{d}z^+ + \mathrm{d}z^-)}$$

where $\mathrm{d}y^+$, $\mathrm{d}y^-$, etc. are the grid spacings in the forward and reverse directions and $\nu_{x,y}$ are the eddy viscosity components used to calculate shear stress from the second derivatives of velocity. Use of the correct finite-difference approximations is important: the solutions are significantly different if the effects of the irregular grid are ignored and the usual regular grid finite-difference operators are used.

Equation 12 is used to iterate towards a solution, updating the velocity at each point with a weighted average of the values at its neighbours. Source terms (Equation 7) are calculated every ten iterations; this was found to improve stability and speed up convergence. The solution is assumed to have converged when the root mean square change in velocity between iterations is less than 1×10^{-6} m/s. Further iterations beyond this were found to not affect the solution by more than $\sim 10^{-3}$ m/s.

2.3 Two-dimensional wall function solution for channels of arbitrary cross-section

While the irregular grid approach described in Section 2.2 works well (see Section 3.2), it is very difficult to apply to non-rectangular cross-sections. The irregular grid approach relies on model grid points close to the wall to represent the steep velocity gradients there but, for non-rectangular channels, arranging the grid in such a way as to capture this near-wall behaviour becomes difficult or even impossible. Instead, another approach has been adopted, which allows the use of a regular grid, while still allowing the model to represent the effects of steep velocity gradients near the bed and walls.

The wall function approach has been used in many previous computational fluid dynamics (CFD) models (Wilcox, 1998), and works by specifying a wall shear stress with the condition that the shear stress is approximately constant near the wall. Equation 9 shows that this assumption is valid for small grid spacings, since the shear stress near the wall is approximately equal to the weight of the water column. The condition of approximately constant shear stress can be expected to hold for other geometries in the region near the bed and walls. Solution of Equation 9 gives the well-known logarithmic velocity distribution near a wall with uniform shear stress, with a profile given by

14.
$$u = \frac{u^*}{\kappa} \log\left(\frac{z}{h_0}\right)$$

where u^* is the shear velocity, equal to $(\tau_b/\rho)^{1/2}$. For this model, a slightly different approach to the standard wall function is used: Equation 14 is used to calculate the ratio of the velocities in the cells next to the wall and the cell above

$$u_0 = \alpha u_1$$

15.
$$\alpha = \frac{\log(2\Delta z/h_0)}{\log(\Delta z/h_0)}$$

Equation 15 is then combined with Equation 12 to allow the velocities u_0 and u_1 to be calculated when combined with the Jacobi solution for the rest of the grid. This means that the shear stress near the wall is not calculated explicitly.

3. Results

3.1 Flow over a planar bed

The Runge–Kutta model was tested for a range of depths between 0·25 and 5 m and for four values of roughness in the range 0·002 to 2 m. While the concept of a roughness height larger than the depth of the channel itself may appear nonsensical it should be borne in mind that this is not a direct physical parameter (Morvan *et al.*, 2008) and, as the zero-velocity depth is equal to $0·033k_s$, a solution can still be derived. All tests used the same slope of 0·001, as varying this was found to produce the expected square root dependence and hence no further testing of the model's response to changes in slope was necessary.

The predicted depth-averaged velocities are shown in Figure 2. The averages were calculated using area weighting to allow for the irregular grids rather than simply an arithmetic mean of the values at each model point. A power law was fitted to the results for each roughness of the form
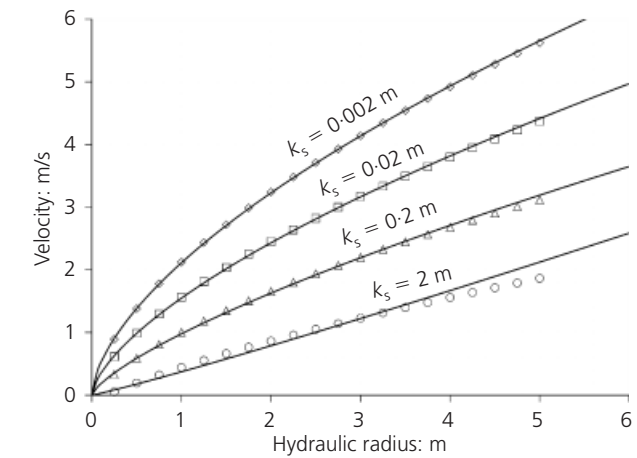
Figure 2. Velocity–hydraulic radius relationship as predicted by the Runge–Kutta solution for flow over a planar bed, for roughness heights in the range 0·002–2 m. The best fit power law relationship for each roughness is shown as a solid line

16.
$$v = \frac{1}{n'} R^\gamma S^{1/2}$$

which can be viewed as a generalised Manning's equation, with the hydraulic radius exponent no longer fixed at 2/3. Table 1 shows the generalised Manning's resistances and exponents for the mixing length models, along with those produced by fitting Equation 16 to the results of the Colebrook–White equation. The fit for $k_s = 2$ m is less good than for the other values of k_s, but is still within ~10%.

The first thing to note is that the exponent of the Colebrook–White equation varies with roughness, but that for Manning's n values typical to natural channels ($n \sim 0·03$), the exponent of 0·734 is close to the value of 2/3 used in Manning's equation. Secondly, values of γ and n' agree well between the mixing length model and the Colebrook–White equation. This shows that the mixing length model is able to reproduce the

Geometry	Aspect ratio	Model	γ				n'			
			$k_s = 0.002$	$k_s = 0.02$	$k_s = 0.2$	$k_s = 2.0$	$k_s = 0.002$	$k_s = 0.02$	$k_s = 0.2$	$k_s = 2.0$
All		Colebrook–White	0·612	0·651	0·734	1·08	0·0150	0·0204	0·0323	0·0848
Planar bed		Runge–Kutta	0·599	0·647	0·724	0·949	0·0141	0·0218	0·0353	0·0895
Circular		Runge–Kutta	0·604	0·657	0·745	1·03	0·0137	0·0209	0·0333	0·0807
Rectangular	2	2D rectangular	0·634	0·669	0·756	1·04	0·0137	0·0188	0·0307	0·0766
Rectangular	5	2D rectangular	0·637	0·670	0·761	1·06	0·0139	0·0191	0·0314	0·0806
Trapezoidal	5	2D wall function	0·615	0·657	0·750	1·05	0·0137	0·0188	0·0301	0·0747

Table 1. Parameters for the best-fit power law relationship of the form $v = (1/n')R^\gamma S^{1/2}$ for the different models and geometries tested

behaviour of the empirically based Colebrook–White equation in predicting average velocities. This does not, however, mean that the velocity profile predicted by the mixing length model is correct.

The predictions of the mixing length model and the Colebrook–White equation also agreed well for circular cross-section channels.

3.2   Flow in a rectangular channel

Figure 1 shows a cross-section with contours of equal streamwise velocity as predicted by the 2D model operating on an irregular grid. All simulations used a grid spacing increment factor (see Section 2.2) of 1·2. As expected, the solution shows an approximately logarithmic profile near the walls and bed (steep velocity gradients), with lower gradients further away from the wall where the flow is well mixed because of longer mixing lengths (smaller velocity gradients).

The fitted power law parameters of Equation 16 are shown in Table 1 for rectangular channels with aspect ratios (width to depth) of 2 and 5. Again, they show good agreement with the Colebrook–White equation. This model is slow, taking 7 min to converge for the irregular grid model applied to a channel 2 m deep, 10 m wide and with a roughness height of 0·2 m. Run times are longer for larger channels and with smaller roughness heights, since the roughness height specifies the initial spacing of points near the bed, producing more grid points in total. There are two reasons for the slow convergence. Firstly, the Jacobi algorithm is notoriously slow to converge and, secondly, Python is not the fastest of languages for numerical programming. A much faster solution would be expected if a solver able to produce a full matrix solution at each iteration were used (analogous to an implicit time-stepping scheme rather than the explicit scheme used here) and the model were reprogrammed in a quicker language such as C or Fortran.

3.3   Flow in a trapezoidal channel

The results of Table 1 show further agreement with the Colebrook–White equation for a trapezoidal channel of aspect ratio 5, with walls of 1:1 slope, when the wall function approach is used to model the velocity profile near the bed. All simulations used a grid spacing such that there are ten grid points in a vertical profile and the horizontal spacing is the same. As a further check of the validity of the wall function approach, it was applied to rectangular channels and compared with the results of the irregular grid model, which could be expected to better represent the velocity profile near the bed and walls. Results from the wall function model give the same level of agreement with the Colebrook–White formula as the other solutions.

3.4   Flow in a compound channel

The wall function model was applied to a compound channel of cross-section shown in Figure 3, using a grid spacing of 0·2 m. Manning's equation is not directly applicable here, since the velocity in the channel is not approximately uniform, but this test does demonstrate that the model is applicable to more complex geometries. Significant horizontal shear is predicted on the floodplain near the banks, with velocity gradients in a horizontal direction approximately 20% of the vertical gradients near the bed in the channel. This is in keeping with our understanding of compound channels (Knight and Shiono, 1996) where shear layers have been observed to develop in the bank regions.

4.   Discussion and conclusions

The results from the model testing are summarised in Figures 4 and 5. Figure 4 shows the velocity–hydraulic radius relationships predicted by the model for all geometries and by the Colebrook–White equation. Figure 5 plots the velocities from all models and geometries against those predicted by the Colebrook–White equation, along with the ideal 1:1 relationship. The mixing length model appears to be capable of reproducing the behaviour of the Colebrook–White and Manning equations for a wide range of
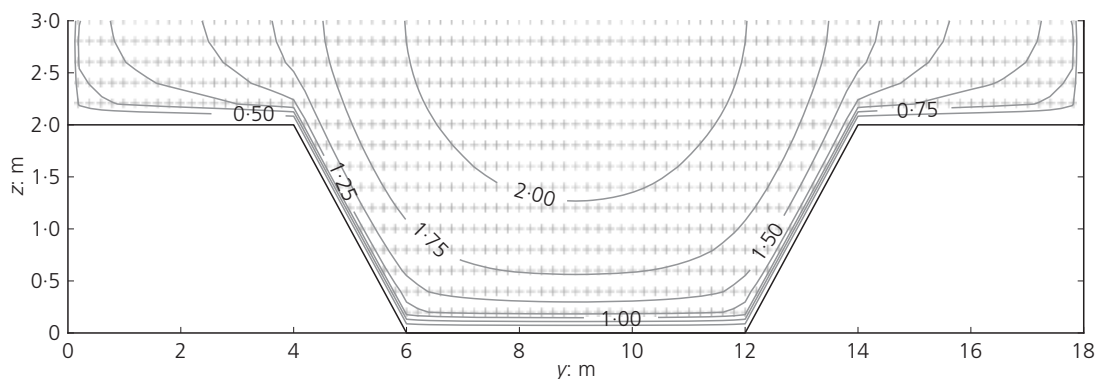
Figure 3. Velocity contours predicted by the mixing length model for a compound channel, using regular grid spacing and the wall function approach. Grid points are shown by crosses
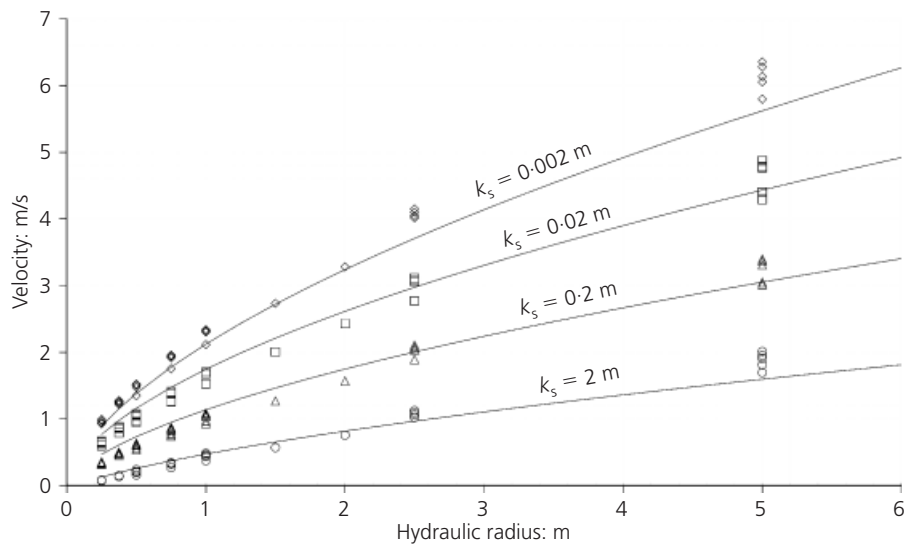
Figure 4. Summary of velocity–hydraulic radius for all mixing
length models (as shown by circles, triangles, etc.). Solid lines
show the v–R relationship predicted by the Colebrook–White
equation
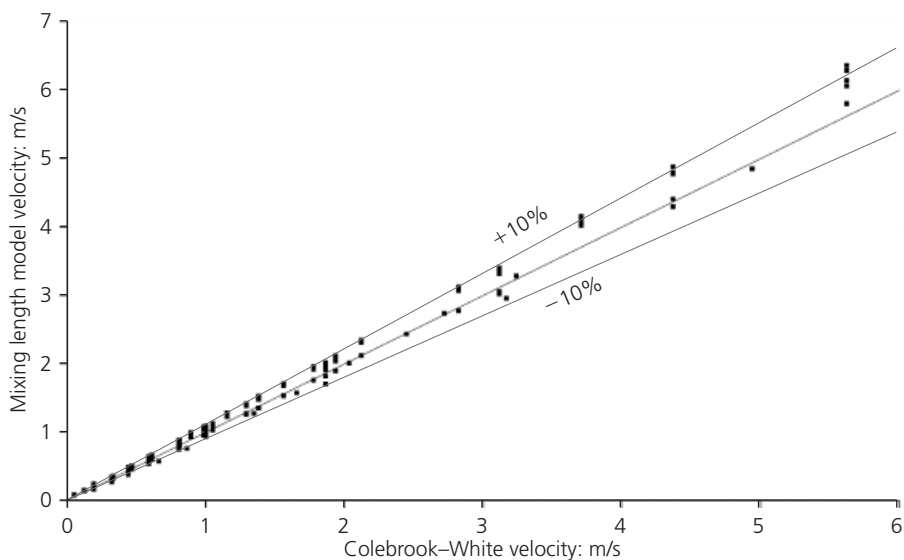
Figure 5. Average velocity predicted by the mixing length model
against that predicted by the Colebrook–White equation, for all
geometries. The 1:1 relationship with $\pm10\%$ is also shown

hydraulic radii and roughness values. 80% of the points lie within
$\pm10\%$ of the 1:1 line, implying that the relative standard error is
<10% (for an error of $\pm10\%$, ~70% would be expected within
these bounds). There is a bias of ~5%, with the mixing length
model generally predicting higher velocities than the Colebrook–
White equation.

For typical natural channel roughnesses, the fitted exponents γ in

the range 0.65–0.76 agree reasonably with the 2/3 exponent of
Manning's equation. It should also be noted that the value
remains similar across the range of geometries, which indicates
that the parameter of hydraulic radius appears to capture the
effect of geometry well.

The results show that the mixing length model performs well in
reproducing some of the well-known hydraulic behaviours of

open channel flows, and can explain how essentially empirical results such as those of Manning and Colebrook–White arise from open channel hydraulic processes. As well as being able to reproduce the known dependence of mean velocity on channel geometry, the mixing length model produces further information such as velocity profiles and bed shear. After these have been validated, they may be of use in practical applications such as sediment transport modelling and estimating scour. Furthermore, Manning-type models are limited to application to simple geometries or by extension to more complex geometries represented as a series of regions, to each of which Manning's equation is applied with no interaction between the regions. The mixing length model offers not only an opportunity to model these complex geometries in a way that is consistent with our understanding of the hydraulics of simple situations, but also models interactions between different regions of the cross-section.

We should not go too far in assuming that the mixing length model can explain the hydraulic behaviour of open channels completely. The model shows some promise in predicting cross-section average velocities, but its ability to predict velocity distributions has not been tested. In particular, the model does not represent secondary flows, which have long been known to significantly affect velocity profiles in straight channels. For example, secondary flows are known to advect faster-moving fluid into corner regions (Gessner, 1973) and therefore velocities predicted by the mixing length model described here must be suspect near corners. The model has also only been applied to steady, uniform flows (as also assumed for Manning's equation, etc.) and only to simple cross-sections. There is the potential to apply the mixing length model to more complex geometries through implementation in other 2D and 3D CFD models (and indeed some models already have this capability), meaning it may be possible to model longer reaches than with more complex turbulence schemes. This offers the opportunity of understanding the physical basis of the way Manning's coefficient is used in engineering practice, where a lumped value of n is used to represent the effects of channel roughness, geometry and other processes such as secondary circulation, interactions with vegetation, hydraulic effects of non-uniform and unsteady flows etc.

Further work is needed to test if the model is successful in recreating velocity distributions seen in laboratory or natural channels and to investigate whether it is applicable to non-uniform flow conditions and more complex geometries. To make this practicable, further work on improving the model speed is also required. There may also be opportunities to use the mixing length approach described here to generate conveyance look-up tables for use in 1D models, in a way similar to the conveyance estimation system (McGahey *et al.*, 2008).

As well as providing a fundamental insight into one of the most frequently used formulae in hydraulic engineering, there is potential for many practical applications of this method of modelling turbulence in open channels. For situations where accurate estimation of channel capacity, such as flood risk assessment, developing or reviewing rating curves for gauging stations, channel design etc., the model may offer advantages over conventional approaches for complex geometries where interaction between zones of different velocity is important. The simplicity of the mixing length model means that it may be applicable to models at a scale larger than current CFD schemes, for example at reach length and for out-of-bank flows. The model could also be used to model head loss through structures, bridges etc., but further development is needed to integrate it into a model of non-uniform flow conditions. The potential of the model (as yet untested) to predict velocity profiles within the channel and bed shear could be used to estimate scour and sediment transport. In this research, the mixing length model has been applied to momentum transfer only, but it can also be used to represent the transport of other fluid properties such as temperature and solute concentration. Models such as the one described here could therefore be of use in estimating the diffusion of pollution and temperature from outfalls, etc.

REFERENCES

Abril JB and Knight DW (2004) Stage–discharge prediction for rivers in flood applying a depth-averaged model. *Journal of Hydraulic Research* **42(6)**: 616–629.

Chanson H (1999) *The Hydraulics of Open Channel Flow.* Butterworth-Heinemann, Oxford, UK.

Colebrook CF (1939) Turbulent flow in pipes, with particular reference to the transition region between the smooth and rough pipe laws. *Journal of the Institution of Civil Engineers* **11(4)**: 133–156.

Darby S and Thorne C (1996) Predicting stage–discharge curves in channels with bank vegetation. *Journal of Hydraulic Engineering* **122(10)**: 583–586.

De Cacqueray N, Hargreaves DM and Morvan HP (2009) A computational study of shear stress in smooth rectangular channels. *Journal of Hydraulic Research* **47(1)**: 50–57.

Gessner FB (1973) The origin of secondary flow in turbulent flow along a corner. *Journal of Fluid Mechanics* **58(1)**: 1–25.

Knight DW and Abril JB (1996) Refined calibration of a depth-averaged model for turbulent flow in a compound channel. *Proceedings of the Institution of Civil Engineers – Water, Maritime and Energy* **118(3)**: 151–159.

Knight DW and Shiono K (1996) River channel and floodplain hydraulics. In *Floodplain Processes* (Anderson MG, Walling DE and Bates PD (eds)). Wiley, London, UK, pp. 139–181.

Lo TS, L'vov VS, Pomyalov A and Procaccia I (2005) Estimating von Kármán's constant from homogeneous turbulence. *Europhysics Letters* **72(6)**: 943–949.

Manning R (1891) On the flow of water in open channels and pipes. *Transactions of the Institution of Civil Engineers of Ireland* **20**: 161–209.

McGahey C, Samuels PG, Knight DW and O'Hare MT (2008) Estimating river flow capacity in practice. *Journal of Flood Risk Management* **1(1)**: 23–33.

Morvan HP, Knight DW, Wright NG, Tang XN and Crossley AJ (2008) The concept of roughness in fluvial hydraulics and its formulation in 1-D, 2-D and 3-D numerical simulation models. *Journal of Hydraulic Research* **46(2)**: 191–208.

Nikuradse J (1933) *Stromungsgesetze in Rauhen Rohren*. VDI Forschungsheft 361, Berlin, Germany.

Prandtl L (1945) Uber ein neues formelsystem für die ausgebildete turbulenz. *Nachrichten der Akademie der Wissenschaften in Göttingen, Mathematisch-Physikalische Klasse*, pp. 6–19.

Press WH, Flannery BP, Teukolsky SA and Vetterling WT (2007) *Numerical Recipes: The Art of Scientific Computing*, 3rd edn. Cambridge University Press, Cambridge, UK.

Rodi W (1993) *Turbulence Models and Their Application in Hydraulics: A State-of-the-art Review*. Taylor & Francis, London, UK.

Schlichting H, Gersten K, Krause E and Oertel HJ (2004) *Boundary-layer Theory*. Springer, Berlin, Germany.

Shiono K and Knight DW (1991) Turbulent open-channel flows with variable depth across the channel. *Journal of Fluid Mechanics* **222**: 617–646.

Wilcox DC (1998) *Turbulence Modeling for CFD*, 2nd edn. DCW, La Cañada, CA, USA.

Yen BC (1991) Hydraulic resistance in open channels. In *Channel Flow Resistance, Centennial of Manning's Formula* (Yen BC (ed.)). Water Resources Publishers, Littleton, CO, USA, pp. 1–135.